Electronic supplementary information

Low-cost laser-cut patterned chips for acoustic concentration of micro to nano particles and cells by operating over a wide frequency range

Jingui Qian[a], Wei Huang[b], Renhua Yang[a], Raymond H. W. Lam[b] and Joshua E.-Y. Lee[*, a, c]

[a]Department of Electrical Engineering, City University of Hong Kong, Hong Kong SAR, China

[b]Department of Biomedical Engineering, City University of Hong Kong, Hong Kong SAR, China

[c]State Key Laboratory of Terahertz and Millimeter Waves, City University of Hong Kong, Hong Kong SAR, China

[*]Corresponding author: josh.lee@cityu.edu.hk

S1 Methods comparing between PnC pattern and periodic structure.

We summarize the merits of our work over the existing method of creating phononic crystals (PnC) on the superstrate to promote particle concentration in the following table.

Table S1 Challenges associated with depending on acoustic band gaps to promote particle concentration and merits of our current work in operating beyond band gaps

	Existing method [1]	**Our work**
Required tool precision^	Very high For 13 MHz* Minimum feature size: 50 μm (tolerance: ±5 μm) For 26 MHz# Minimum feature size: 30 μm (tolerance: ±3 μm)	Rather low Minimum feature size: 100 μm (for frequencies up to 26 MHz)
SAW device IDT period design	Fixed, must match the PnC designed acoustic band gap	No matching required
Design process of patterned structures on superstrate	Several iterations of simulations to engineer required band gap	Only design requirement is to have a low fill factor
Fabrication method of superstrate	Microfabrication (lithography and DRIE)	Laser-cutting or other suitable tools
Cost of disposable superstrate	Costly, need lots of clean room facilities	Low cost, rapid prototyping options available
Operation frequency	Limited range set by band gaps	Wide range: 7-30 MHz
Applicable to other materials?	Unknown. Must be considered case-by-case for each material.	Yes
Superstrate must be aligned to SAW device?	Yes	No need

*Wafer must be thinned down to 200 μm otherwise no acoustic band gap would exist for any chosen lateral dimensions for the PnC design and based on an expected SAW frequency uncertainty of ± 0.5 MHz.
#Wafer must be thinned down to 100 μm otherwise no acoustic band gap would exist for any chosen lateral dimensions for the PnC design and based on an expected SAW frequency uncertainty of ± 1 MHz.

As can be seen from the table, the required tooling precision to ensure the SAW frequency lies in a designed acoustic band gap is beyond the capability of laser cutting.

S2 Design parameters of periodic structures and simulated acoustic band gaps (longitudinal direction).

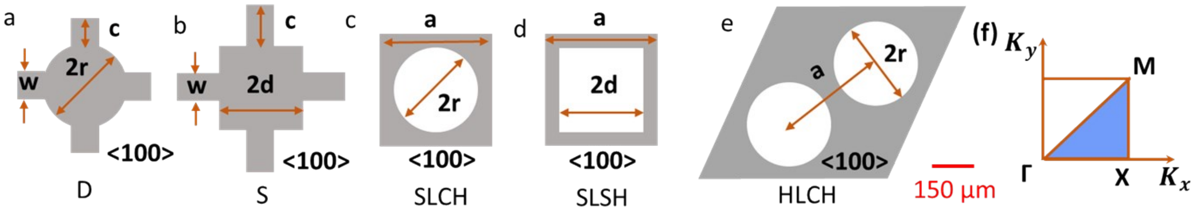

Fig. S1 Schematic of unit cells of the five kinds of periodic structures considered.

Table S2: Design parameters of the periodic structures and simulated acoustic band gaps.

Unit cell design	a (μm)	w (μm)	r (μm)	c (μm)	d (μm)	Band gaps	BGR	Fill factor
D	-	50	150	50	-	5.09-7.45 MHz, 9.62-10.42 MHz	37.6% 8%	50.4%
S	-	50	-	75	150	4.08-6.5 MHz, 7.25-7.84 MHz, 8.66-8.95 MHz	45.7% 7.8% 1.8%	51.85%
SLCH	400	-	150	-	-	None	-	55.84%
SLSH	400	-	-	-	150	None	-	43.75%
HLCH	400	-	150	-	-	5.11-5.60 MHz	9.15%	66.01%

Fill factor is defined as the ratio of the solid area within a unit cell over the total area of the unit cell. BGR refers to the band gap ratio, which is defined as the gap-to-mid gap (i.e. center frequency) ratio, which can be expressed by:

$$BGR = \frac{f_u - f_l}{(f_u + f_l)/2} \tag{1}$$

where the f_u and f_l are the upper and lower bound frequencies respectively.

S3: Simulated dispersion relations of the SLCH and SLSH unit cell designs that show no band gap.

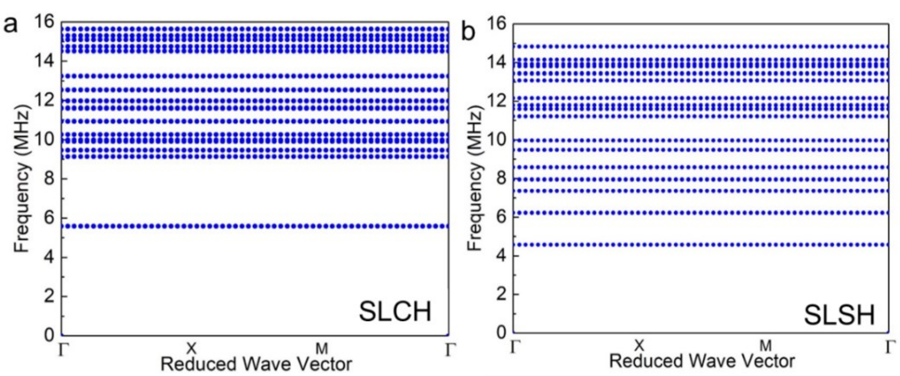

Fig. S2 Simulated dispersion curve of the (a) SLCH and (b) SLSH unit cell design by FE analysis.

S4: Simulation of acoustic wave propagation through periodic structures with some acoustic band gap (D, S and HLCH unit cell designs).

To visualize the filtering function of the three periodic structures with some acoustic band gap, we constructed two-dimensional models (using COMSOL) of the three square plates based on the fabricated superstrate designs. A plane wave was launched from one side of the square plate: a side that is close to the patterned structures. In other words, the effect of transmission through the bottom of the silicon plate was not considered. The plane wave was launched at each of the three frequencies applied in the experiments (i.e. 7.1 MHz, 9.8 MHz, and 13.6 MHz). We simulated the propagation behavior of acoustic waves PnC structure on the propagation of acoustic wave, the asymmetry filter (3 designs of PnC array structures) on a silicon plate was molded in the COMSOL software. The plane wave was with an acceleration was launched from the left side of the silicon plate. The frequencies of the input wave were chosen same as the excitation resonant frequencies of the IDTs. There was acoustic wave's reflection, scattering, and diffraction phenomenon were observed for the different frequencies of the different PnC. When the acoustic wave frequency beyond (both of higher and lower) the BG of PnC unit cell, they could directly pass through the PnC structure with seldom loss. When the acoustic wave frequency within the BG of PnC unit cell, the PnC structure will hinder the acoustic wave propagation and reflect them back.

It should be noted that the simulation was not exactly matched with our two-chip acoustofluidic device, where the acoustic wave was leaked and coupled from the SAW device to superstrate rather than radiated from the left side.

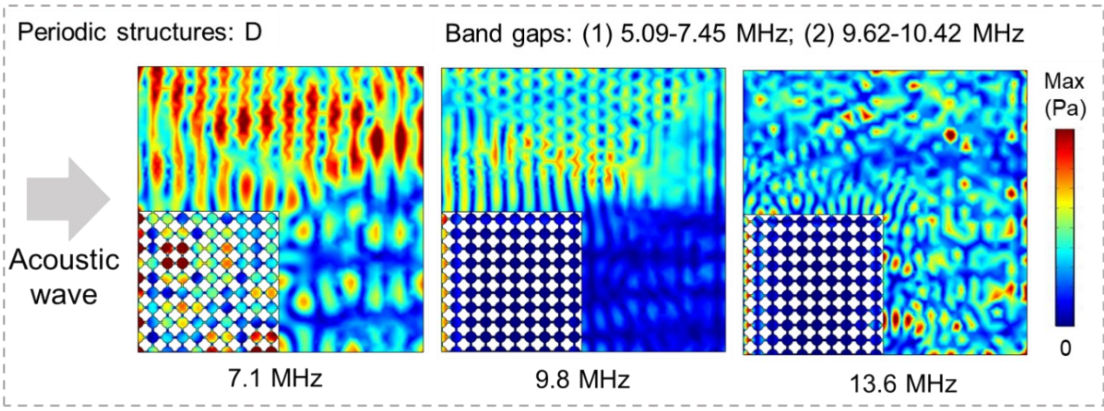

Fig. S3 Simulated acoustic wave intensity on a silicon plate with periodic structures based on D-type unit cell design (theoretical band gaps: 5.09-7.45 MHz, 9.62-10.42 MHz). As shown by the left and middle images, the acoustic wave is prohibited from propagation through the periodic structures at 7.1 MHz and 9.8 MHz (within the acoustic band gap). At 13.6 MHz (i.e. above the band gap), the acoustic wave passes through the periodic structures underhinded.

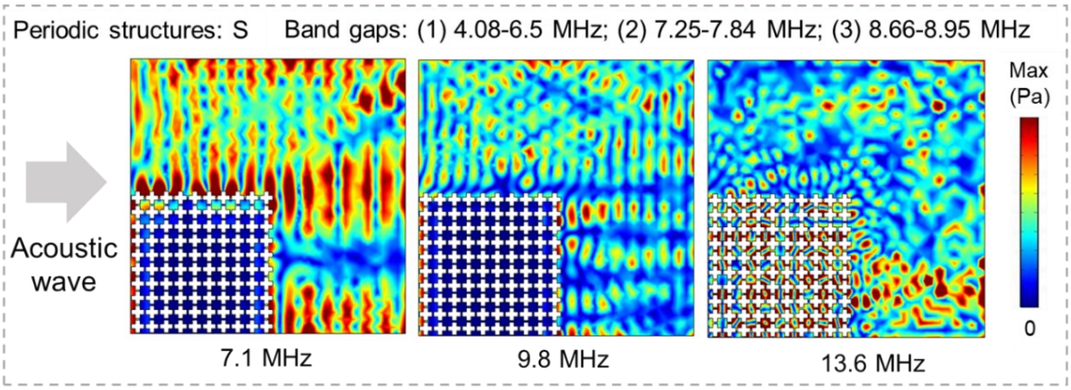

Fig. S4 Simulated acoustic wave intensity on a silicon plate with periodic structures based on S-type unit cell design, where none of the launched wave frequencies lie in the theoretical band gap (4.08-6.5 MHz, 7.25-7.84 MHz, 8.66-8.95 MHz). In all three test frequencies, the acoustic wave passes through the periodic structures underhinded.

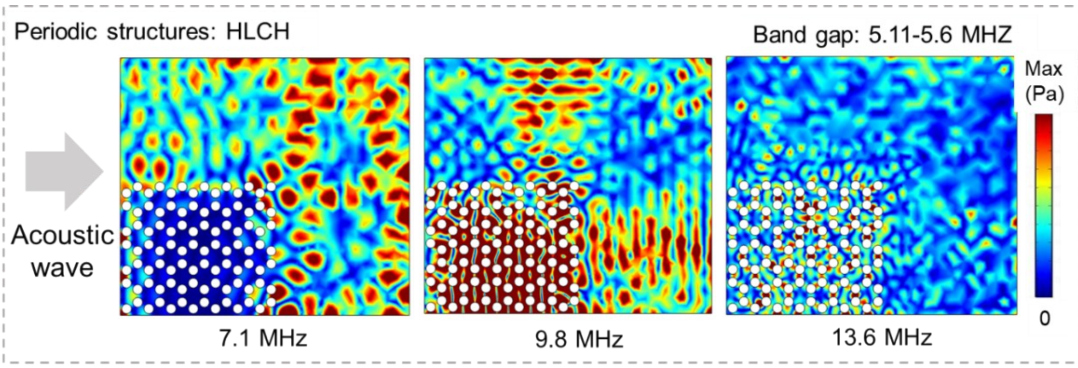

Fig. S5 Simulated acoustic wave intensity on a silicon plate with periodic structures based on HLCH-type unit cell design, where none of the launched wave frequencies lie in the theoretical band gap (5.11-5.6 MHz). In all three test frequencies, the acoustic wave passes through the periodic structures underhinded.

S5 Reflection coefficient S_{11} measurement of the SAW device

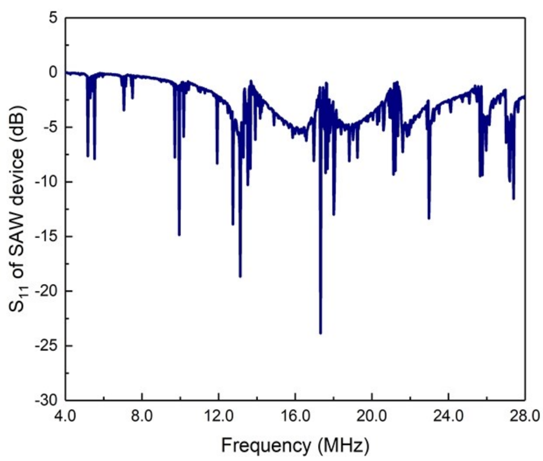

Fig. S6 Measured S_{11} parameter of the fabricated SAW device by network analyzer.

S6 Acoustic force analysis

Particles or cells in a sessile droplet are subjected to both the acoustic streaming force (ASF) and acoustic radiation force (ARF) [1-2]. The formula of the time-averaged value of the ARF can be described by [3-4]:

$$F_R = \pi D^2 Y_R \sin(skx) E \tag{2}$$

Dimensionless ARF factor $$Y_R = \frac{4}{3}\kappa\left(\frac{5\beta - 2}{2\beta + 1} - \frac{1}{\beta\gamma^2}\right) \tag{3}$$

Mean acoustic energy density $$E = \frac{p^2}{2\rho_f {C_f}^2} \tag{4}$$

Dimensionless factor $$\kappa = \frac{2\pi f D}{C_f} \tag{5}$$

Wave number $$k = \frac{2\pi}{\lambda} \tag{6}$$

where, the D is the radius of the particles (or cells), f and C_f are the frequency of acoustic wave and speed of sound in the sample fluid respectively, β is the density ratio of the particle to the fluid, and γ is the sound speed ratio of the particle to the fluid, p and ρ_f are the amplitude of acoustic pressure and density of the sample fluid respectively, x is the distance of the particles from the pressure node, λ is the wavelength of the acoustic wave. Therefore, the amplitude of the ARF is related to the factor κ, which is in direct proportion to the particle size and acoustic frequency (or wavelength). The acoustic pressure could be expressed as:

$$p = p_0 e^{-\alpha x/2} e^{i(kx - 2\pi f t)} \tag{7}$$

$$p_0 = \sqrt{PZ/A} \tag{8}$$

where p_0 is the original acoustic pressure amplitude, α is the attenuation coefficient, P is the input power, Z is acoustic impendence and A is the working area of acoustic field, respectively.

Moreover, the ASF-based drag force was calculated by:

$$F_d = 6D\pi\eta\mu \tag{9}$$

where, the η is the dynamic viscosity of the fluid, μ is the acoustic streaming velocity.

S7: Particle concentration on a periodic-structured superstrate using the next three higher order modes.

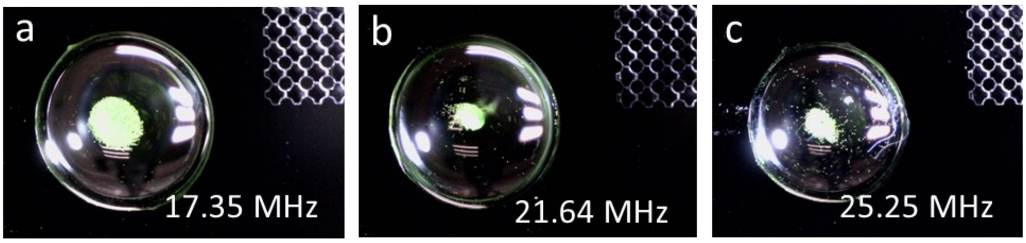

Fig. S7 Particle concentration on a periodic-structured superstrate (D-type unit cell design) using the next three higher order modes (17.35 MHz, 21.64 MHz, and 25.25 MHz).

S8: Particle concentration on a non-patterned silicon superstrate by manual positioning/ misalignment of the superstrate.

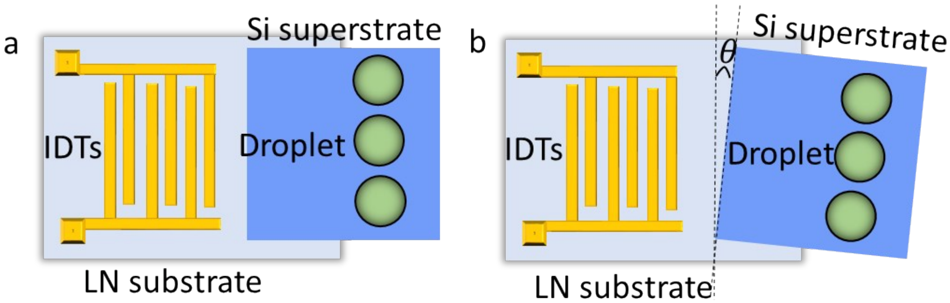

Fig. S8 Two-chip acoustofluidic setup for particle concentration on a non-patterned silicon superstrate where the chip is placed (a) parallel to the IDT fingers (i.e. perpendicular to the incident acoustic wave), and (b) at a slight angle ($\theta \approx 0°$-$30°$) to the IDT fingers.

When the non-patterned superstrate was placed parallel to the IDT fingers, the generated acoustic field is uniform across the aperture of the wave. When rotate the non-patterned superstrate to form a misalign angle with the IDTs fingers, an asymmetric acoustic field is confined within a specific zone on the superstrate due to reflection bias off the edge of the superstrate.

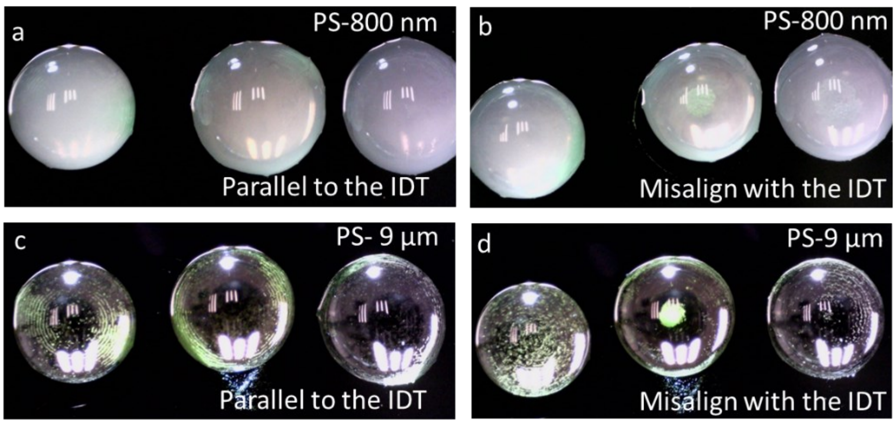

Fig. S9 Results of particles concentration experiments on a non-patterned silicon superstrate (a, c) placed parallel to the IDT fingers, and (b, d) rotated at an angle to the IDT fingers to introduce partial asymmetry to the acoustic field on the superstrate. Labeled values indicate the diameters of the PS particles used.

In the case of placement parallel to the IDT fingers, for both particle sizes tested (800 nm and 9 µm), we see the formation of multi-turn rings around the periphery of droplet. These results indicate that only symmetric acoustic fields were generated. In the case of misaligning at a rotation angle to the IDT fingers, we see particle concentration only in the middle droplet but not so in the other droplets on either side. These results indicate that the asymmetric acoustic field was confined within a specific zone (e.g. central area) of the superstrate, as has also been reported in [5]. It is worth noting that the efficacy of approach is highly sensitive to the combination of two factors: droplet location on the superstrate and rotation angle of misalignment in positioning the superstrate. As such, several iterations of adjustments and tries are required before a successful attempt at droplet concentration is finally recorded. Hence although it is possible to realize particle concentration on non-patterned superstrates, the outcome is highly variable, and the process of setting up is highly time consuming. In the case of what we have proposed with patterned superstrates, the results are highly reliable and reproducible, requiring minimal adjustments.

S9: Particle concentration on periodic-structured superstrates with a misaligned angle to the IDTs.

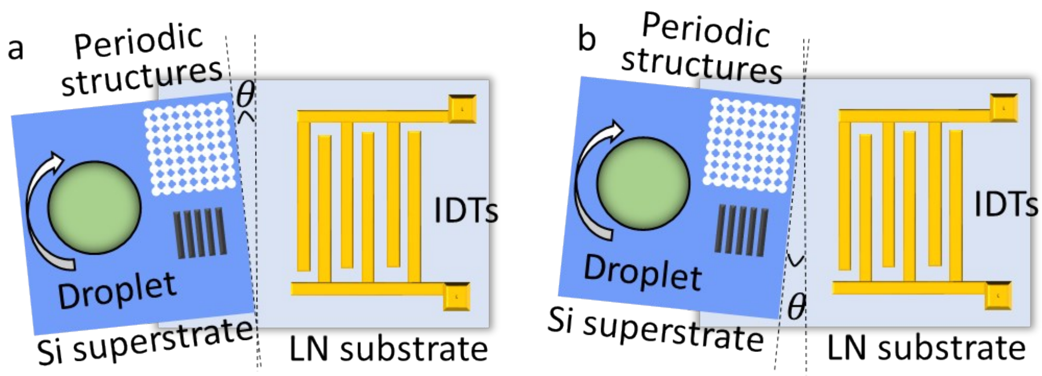

Fig. S10 Two-chip acoustofluidic setup with a periodic-structured superstrate deliberately misaligned to the IDT fingers with the aim of evaluating the effect of misalignment on particle concentration performance. (a) Patterned superstrate rotated by a slight angle anticlockwise. (b) Patterned superstrate rotated by a slight angle rotation clockwise.

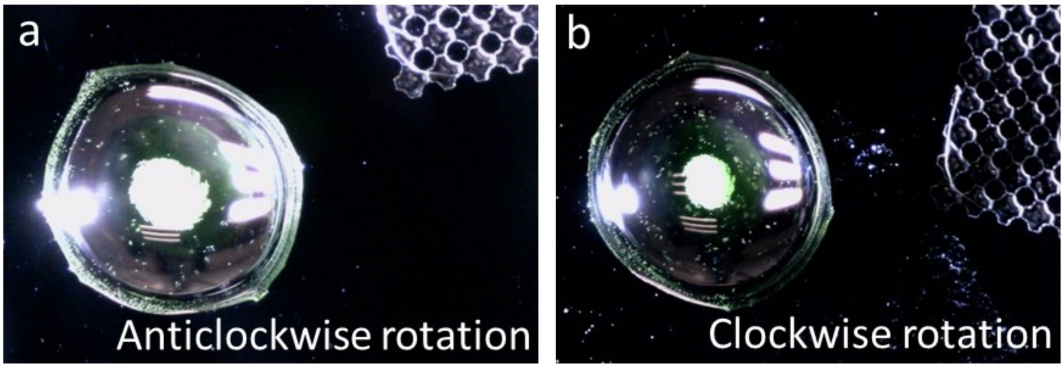

Fig. S11 Particle concentration experiment on a patterned superstrate to assess the effect of misaligned rotation of the superstrate. (a) Patterned superstrate rotated by a slight angle anticlockwise. (b) Patterned superstrate rotated by a slight angle rotation clockwise.

S10: Videos demonstration for particle and cell concentration.

Video S1 Concentration of micro and nano particles in a sessile droplet of DI water.
Video S2 Focusing of tumor cells in a sessile droplet of culture medium.

References

[1] R. Wilson, J. Reboud, Y. Bourquin, S. L. Neale, Y. Zhang and J. M. Cooper, Lab Chip, 2011, 11, 323-328.
[2] G. Destgeer, B. Ha, J. Park and H. J. Sung, Anal. Chem., 2016, 88, 3976-3981.
[3] G. Destgeer, J. H. Jung, J. Park, H. Ahmed and H. J. Sung, Anal. Chem., 2017, 89, 736-744.
[4] Z. Ma, D. J. Collins, J. Guo and Y. Ai, Anal. Chem., 2016, 88, 11844-11851.
[5] J.-C. Hsu and Y.-D. Lin, Sens. Actuator A-Phys., 2019, 300, 111651.
[6] K. S. Wong, L. Lee, Y. M. Hung, L. Y. Yeo and M. K. Tan, Anal. Chem., 2019, 91, 12358-12368.